International Journal for Multidisciplinary Research (IJFMR)
E-ISSN: 2582-2160 ● Website: www.ijfmr.com ● Email: editor@ijfmr.com

Current Controllers for Single-Phase Grid-Connected Inverters: Review and Analysis

Bhagyalakshmi P S[1], Dr. Bos Mathew Jos[2]

[1]Ph. D Scholar, Mar Athanasius College of Engineering, Kothamangalam, Kerala, India[12]
[2]Professor, Mar Athanasius College of Engineering, Kothamangalam, Kerala, India[12]

Abstract:
This paper mainly focuses on multiple current controller methods for a grid-connected inverter-based distributed generation. PI, PR, DQ, and Hysteresis controllers are the different control methods used for the analysis. Switching pulses for the conventional H-bridge inverter are generated, and the output total harmonic distortion analysis is performed using these controllers. Disadvantages of a PI current control include its steady-state errors as well as its extremely low rejection capability. As a solution to the issues of PI controller, PR controller was invented. In addition to the PI and PR controllers, Direct-Quadrature and hysteresis controllers are also studied and compared in terms of total harmonic distortion. Analytical results of the hysteresis current controller are compared with different bandwidths. The performance of these controllers has been examined using MATLAB/Simulink by evaluating the switching frequency and current THD of the inverter.

Keywords: Full bridge inverter, grid-connected inverter, current controllers, PI controller, PR controllers, DQ current controller, Hysteresis controller

1. Introduction

Because of its benefits, such as low carbon emissions, the ability to tap resources in remote regions, and low voltage ride-through capabilities, sustainable energies are becoming more and more significant. There is increased interest in photovoltaic systems (PV) using various DER kinds in microgrids [1]. The introduction of decentralised generating systems makes it possible to replace centralised power plants because there are more renewable energy sources available and there is less pollution from fossil fuels. In distributed generation (DG) systems, voltage-source inverters (VSI) with current-regulated PWM are used to synchronize DG sources with the utility grid. Power electronic semiconductor-based converters are needed to harvest energy from non-conventional energy sources because they are naturally intermittent. In addition, the electrical power generated in the solar and wind energy sectors will not be suitable for direct integration with the current power system [2].

For inverters connected to grids, PWM is the effective method of control. Current-controlled PWM has a number of advantages over open loop voltage PWM converters, including quick dynamic response, built-in over-current prevention, efficient use of dc links and peak current protection. The overall generation of energy has benefited greatly from the control of grid-connected inverters since the incorporation of non-conventional energy resources into systems. The inverter's current regulation is the most difficult aspect of the behaviour of renewable resources connected to the grid.

The type of current control mechanism employed mostly determines the converter system's performance. A PWM modulator receives the errors from the detection of load currents in a current controller and compares them to reference currents to generate inverter switching signals [11]. The literature has provided several methods for controlling current using both linear and nonlinear controllers [3]. Linear controllers based on PWM modulation provide improved steady-state response, depending on the type of connected load.

The inverter is a crucial part of the freestanding PV system. The controller must limit the ripples these inverters produce to deliver a perfect sinusoidal yield and avoid any detrimental effects on the power quality, as the inverter must be controlled in order to provide the load with high-quality output.

2. Single-phase Full Bridge Inverter

There are two topologies for single-phase VSI: half-bridge and full-bridge. One of the primary characteristics of a full-bridge inverter is that its modulating mechanism should always guarantee that the inverter leg's top or bottom switch is on at all times [16].

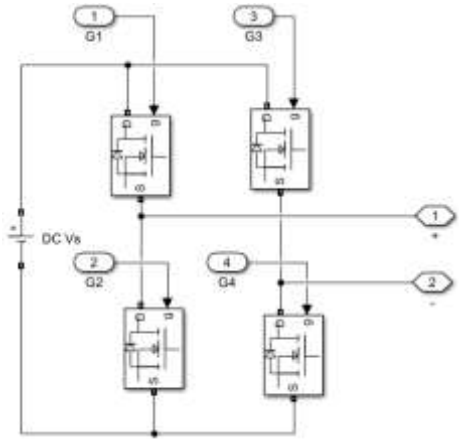

Figure 1. Full Bridge Inverter

Fig. 1 shows the traditional full-bridge inverter circuit. V_{dc} is the input voltage is applied to the inverter. S_1, S_2, S_3, and S_4 switches receive pulses that regulate the inverter's voltage. The voltage differential between the load and reference voltages V_{ref}, determines whether switching pulses are generated [14].

2.1 Grid-Connected Inverter

An AC source, the grid, is linked to the inverter. By utilising a DC-DC Voltage Source Inverter (VSI) and a Boost converter PV system can be connected to the grid.

Two loops formed the control technique: a current loop to manage grid current and consequently enhance the quality of the waveform, and an outside voltage loop to control voltage at the DC link [18]. To supply current to the grid, the inverter voltage needs to be higher than the grid voltage, or the inverter current angle needs to be greater than 90°.

The utility grid and distributed generation are often synchronised using a current-controlled voltage sensing interface (VSI). The voltage that the inverter generates must be higher than the Vg when utilising an inverter-based DG. Ensuring power transmission to the grid is crucial. Since Vg is uncontrollable, the simplest way to regulate the operation is to regulate the current that enters the grid [4]. The entire grid-connected inverter model with current controller loop is displayed in Fig. 2.

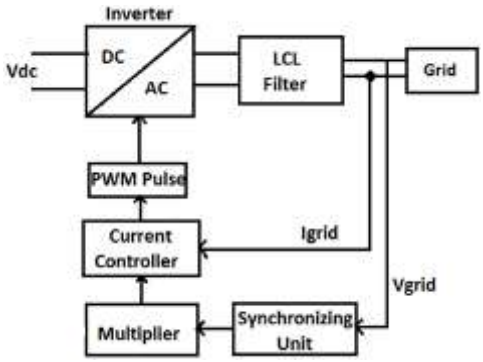

Figure 2. Block diagram of the Closed Loop of the Inverter

3. Current Controllers for Single-Phase Inverter

Controllers are necessary to maintain the rated voltage during load variation. To ensure that the output current given to every load is of a high quality, various control mechanisms have been implemented. Proportional-Integral (PI), Proportional-Resonant (PR), Direct Quadrature (DQ), and Hysteresis current controllers are among the kinds of current regulators that are available. [7].

3.1 PI Controller

The current from the inverter, I_{inv}, is monitored and compared to the reference current, I_{ref}. The grid voltage is sent, then it is converted to reference current to get I_{ref}. The current error, I_e, is provided to a proportional integral controller. Through a reduction in the instantaneous error, the integral component in the PI controller enhances tracking. The resultant error signal is compared to a triangle carrier signal in order to generate PWM signals for the inverter switches.

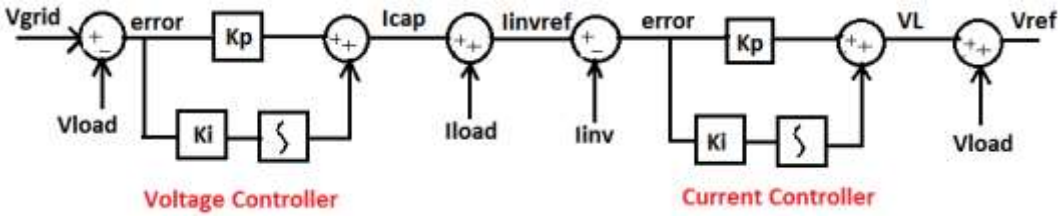

Figure 3. PI Current controller for Closed Loop Inverter

A PI controller processes the difference between the measured and reference currents to generate the reference voltages depicted in Figure 3 [11].

3.2 PR Controller

This controller is primarily used to stabilise the microgrid's voltage and frequency. When compared to another controller, the PR controller is a convincing method to use as a reference because it has no steady state error. Harmonic compensation for the fundamental frequency can be accomplished in addition to this integrator using a cascade controller [1].

$$Y(S) = E(S) * (K_P + \frac{K_r S}{S^2+\omega^2}) \qquad \text{Eq. 3}$$

Eq. (3) provides the general equation that describes the PR controller. Where E(s) represents the voltage difference between the actual and reference voltages, and Y(s) is the controller's reaction [1]. PR controller's primary practical utility is due to its improved capacity to reject disturbances [7]. Fig. 4 shows the PR controller-based current controller as well as the voltage controller for synchronization with the grid voltage and frequency.

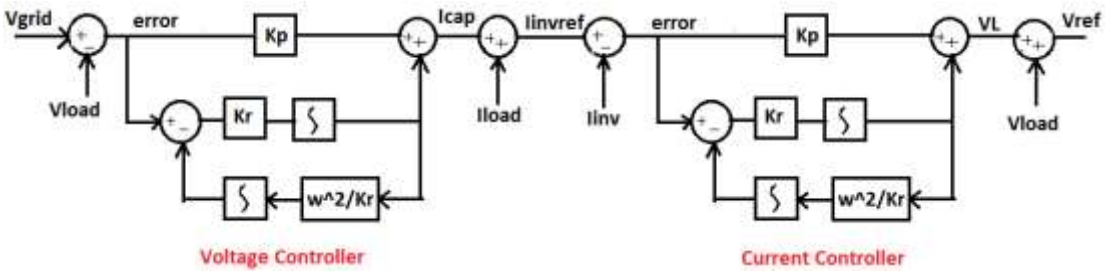

Figure 4. PR Current controller for Closed Loop Inverter

3.3 PR with PLL

The grid-connected inverter uses the phase-locked loop (PLL) functionality in this role. The PLL generates the grid voltage angle, and this angle must be used as the current reference. Here, the PLL is implemented using a low-pass filter [13]. The above PR controller-based voltage controller is replaced by the PLL shown in Figure 5.

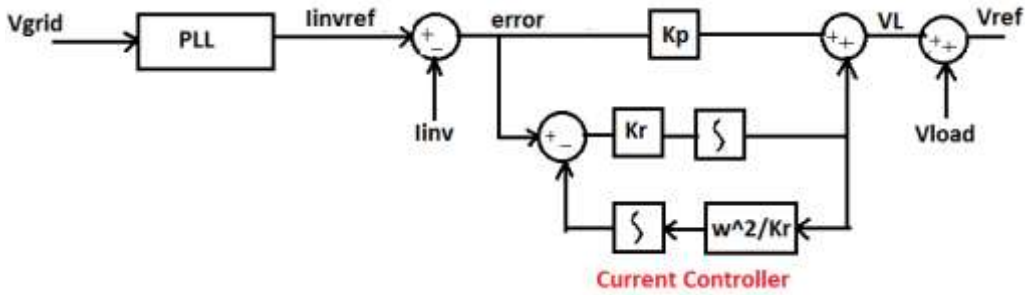

Figure 5. PR Current controller with PLL for Closed Loop Inverter

3.4 DQ Controller

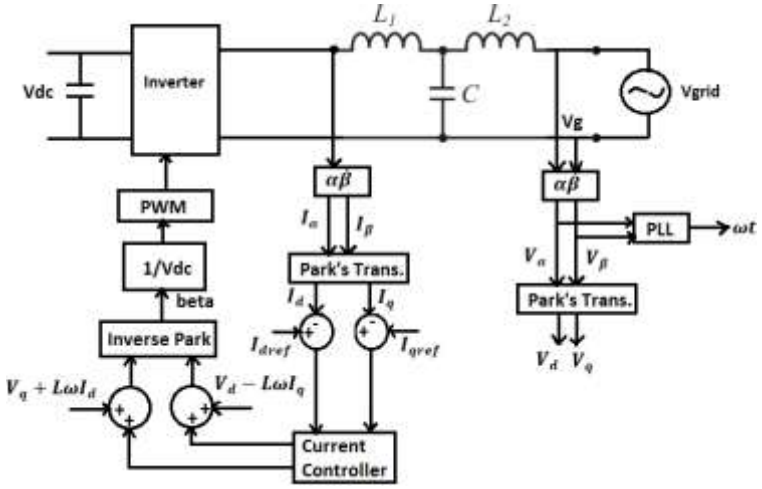

Figure 6. DQ Current controller for Closed Loop Inverter

The dq transformation matrix is as follows,

$$\begin{bmatrix} X_d \\ X_q \end{bmatrix} = \begin{bmatrix} cos\theta & sin\theta \\ -sin\theta & cos\theta \end{bmatrix} \begin{bmatrix} X_\alpha \\ X_\beta \end{bmatrix} \quad \text{Eq. 4}$$

The orthogonal signal generation SOGI technique serves as the foundation for this block. When the inverter is functioning efficiently in current-controlled mode, current control can be obtained through the

inner control loop. To directly control the active and reactive power, power control is implemented in the outer loop, where reference values are provided or the voltage at the DC connection is adjusted.

To keep the converted dq frame signals in sync with the grid, phase-locked loops, are employed to continuously measure the phase of the grid voltage. The dq and inverse transformations are performed using the phase of the grid voltage by the PLL, as shown in Figure 6 [2].

The letters V_i, V, and I are the inverter voltage, grid voltage, and injected current, respectively. The dq transformation on V_i can then be used to generate the next two equations [2].

$$L\frac{di_d}{dt} + Ri_d - \omega Li_q = V_{d1} - V_d \qquad \text{Eq. 5}$$

$$L\frac{di_q}{dt} + Ri_q - \omega Li_d = V_{q1} - V_q \qquad \text{Eq. 6}$$

i_d = direct current component, i_q = quadrature current component, V_{d1} = inverter direct voltage component, V_{q1} = inverter quadrature voltage component, V_d = grid side direct voltage, V_q = grid side quadrature voltage and ω = angular frequency of grid voltage.

Let V_{d1} and V_{q1} serve as the representation of the dq frame transformed components of the reference output voltage [2]. They are given as follows,

$$V_{d1}^{*} = V_{d1} + \omega Li_q - V_d \qquad \text{Eq. 7}$$

$$V_{q1}^{*} = V_{d1} - \omega Li_q - V_q \qquad \text{Eq. 8}$$

$$L\frac{di_d}{dt} + Ri_d = V_{d1}^{*} \qquad \text{Eq. 9}$$

$$L\frac{di_q}{dt} + Ri_q = V_{q1}^{*} \qquad \text{Eq. 10}$$

By altering the output of the current loop to be V_{q1}^{*} & V_{d1}^{*}, we can now absolutely see that the current direct and quadrature components will only be dependent upon the components of the inverter voltage reference signal. Once these Vq1* & Vd1* components have been created, the generated reference signal is needed to produce switching pulses by doing an inverse dq transformation.

3.5 Hysteresis Controller

Hysteresis current controllers (HCC) are among the techniques that offer quick dynamic response, simplicity in implementation, and robustness to changes in output load parameters. In [3], many HCC strategies have been proposed for grid-connected systems. Based on the bipolar and unipolar output voltage of the inverter, two types of hysteresis control (HCC) are available: single-band hysteresis control (SBHCC) and double-band hysteresis control (DBHCC). Performance is assessed using THD and the maximum switching frequency (Fswmax). [7].

3.5.1 Single-band Hysteresis Controller

A bipolar output is produced at the SBHCC inverter's output. The design's structure is shown in Fig. 7. Two switches of a single-phase inverter (Fig. 1) will emit a switching pulse when the error exceeds the hysteresis band (HB). Equations (1) and (2) in the case of an inverter, defined for each pair [3].

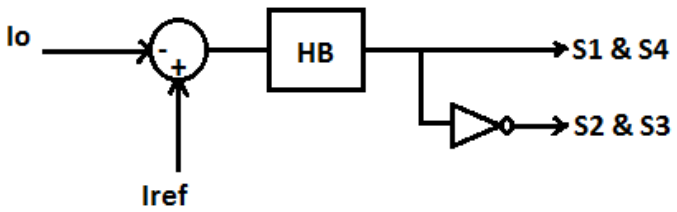

Figure 7. Single Band Hysteresis Controller

$$e = I_0 - I_{ref}$$

The following is the formulation of the switching pulse:
S1 and S4 are switched on if e > HB.
If S2 and S3 are switched on by e <-HB.

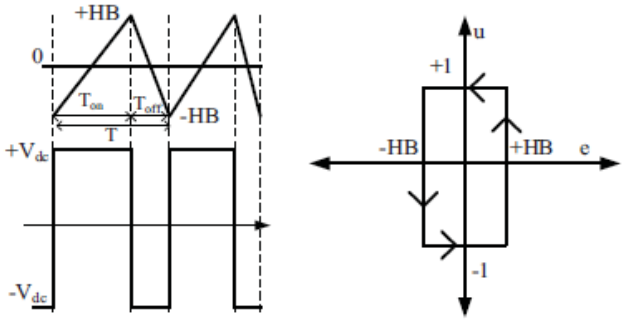

Figure 8. Algorithm for Single-Band Hysteresis Controller

$$f_{SSB} = \frac{V_{dc}{}^2 - V_g{}^2}{4V_{dc} * L * HB} \quad \text{Eq. 11}$$

$$f_{SSB_{max}} = \frac{V_{dc}{}^2}{4V_{dc} * L * HB} \quad \text{Eq. 12}$$

The main issue of the SBHCC is its higher switching losses, as a result of high switching frequency. Raising the bandwidth can decrease switching losses; however doing so will increase current distortion [10].

3.5.2 Double band hysteresis controller

Two main DBHCC techniques are discussed in [2] [6]. The switching pulses need two hysteresis bands to be produced [3]. The main benefit of the DBHCC scheme is that the switching loss is decreased when the switching frequency is lowered. A further benefit of the DBHCC scheme is that, for the same parameters, the inverter's output current exhibits less distortion when compared to the SBHCC scheme.

3.5.2.1 DBHCC-1

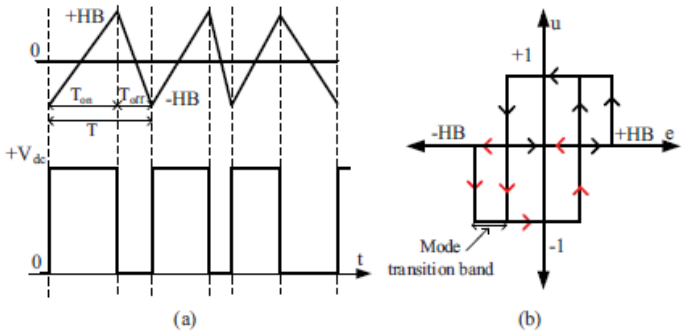

Figure 9. Algorithm for Double Band Hysteresis Current Controller

This control method works by using a smaller hysteresis band to control one set of switches within a single-phase leg inverter and a larger hysteresis band to control a different pair of switches. A narrower hysteresis band determines the invalid signal band. This band's primary function is to switch the outputs from positive to negative and from negative to positive.

$$T_{on} = \frac{2HB * L}{V_{dc} - V_g} \quad \text{Eq. 13}$$

$$T_{off} = \frac{2HB * L}{V_g} \quad \text{Eq. 14}$$

$$T_{S_{DB-1}} = \frac{2V_{dc}*L*HB}{(V_{dc}-V_g)*V_g} \quad \text{Eq. 15}$$

Switching frequency for DBHCC-1 is as follows,

$$f_{S_{DB-1}} = \frac{(V_{dc}-V_g)*V_g}{2V_{dc}*L*HB} \quad \text{Eq. 16}$$

3.5.2.2 DBHCC-2

The typical hysteresis band is divided into -HB to 0 and 0 to +HB rather than –HB to +HB to minimise the switching losses and to enhance the harmonic distortion of the inverter current [12]. The three levels of the DBHCC regulate the PWM-VSI's output current. Here, the voltage of the input DC connection is adjusted from +VDC to 0 and 0 to -VDC [10]. The hysteresis band is split into levels, from –HB to 0 and 0 to +HB, as shown in Fig. 10. The equation below shows the DBHCC switching frequency calculation.

$$T_{on} = \frac{HB*L}{V_{dc}-V_g} \quad \text{Eq. 17}$$

$$T_{off} = \frac{HB*L}{V_g} \quad \text{Eq. 18}$$

$$T_{S_{DB-2}} = \frac{V_{dc}*L*HB}{(V_{dc}-V_g)*V_g} \quad \text{Eq. 19}$$

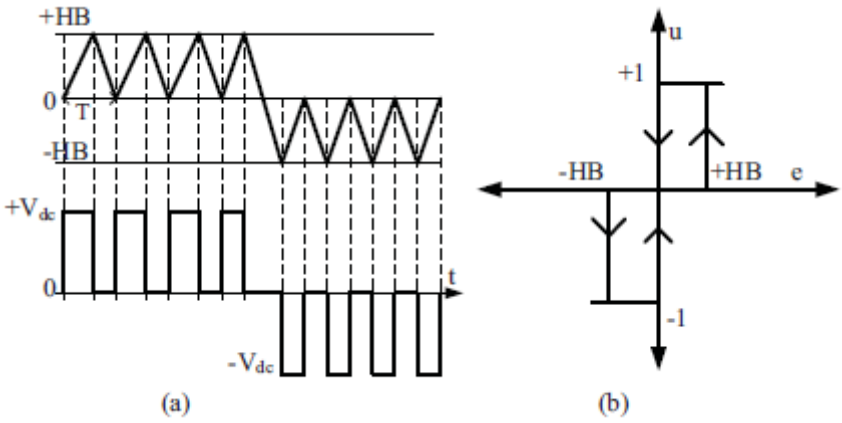

Figure 10. Algorithm for Double Band Hysteresis Current Controller

As seen in Figure 10, the output voltage for DBHCC-2 is obtained with the transition of the error signal from 0 to +HB. Thus, the equation for switching frequency should be twice that of DBHCC-1.

$$f_{S_{DB-2}} = \frac{(V_{dc}-V_g)*V_g}{V_{dc}*L*HB} \quad \text{Eq. 20}$$

A zero level is added to the output as a result of the hysteresis band change, which lowers the switching frequency. This altered structure also lowers THD [12].

4. Analysis and Discussions

Table 1 Simulation parameter

Parameter	Values
Switching Frequency f_s	20 kHz
Output Power	20Watts
DC link Voltage	40V
Inverter side filter Inductance L_1	1.77 mH

Filter Capacitance C	7.96 μF
Grid side filter Inductance L_2	1.41 mH

Simulation of the open-loop inverter is carried out in MATLAB/Simulink software. Table 1 shows a list of components used for the simulation. DC voltage source V_{dc} = 40 V, rms grid voltage V_g = 20 V, resistance R = 20Ω, reference current, i_{ref} = 1.414 sin(314t) A, and sampling frequency f_s = 20kHz. LCL filter is simulated for filtering purposes, and it is designed with a ripple in current having 20% output current as follows.

4.1 Open Loop Inverter

In single-phase inverters, the electrical current is switched by four MOSFETs. The two MOSFETs (S_2 & S_3) will operate for the lower half cycle of the sine wave, while the other two MOSFETs (S_1 & S_4) will work for the upper half cycle. This allows us to create a square wave AC output. But our appliances cannot be used with this source.

Simulation of open-loop inverter was performed for an input voltage of 40V, having 20 kHz as the switching frequency to get the 20V rms voltage at the output shown in Fig. 11. So the voltage at the output is obtained as 31.7V and the current of 1.6A with a 50Hz fundamental frequency, shown in Fig. 12. For this, the THD of the load current is given as 2.55%.

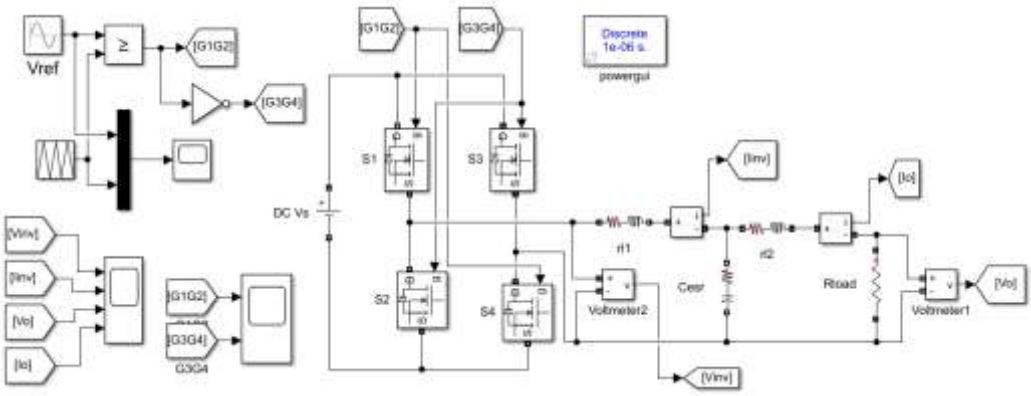

Figure 11. Simulink Model of Open-Loop Inverter

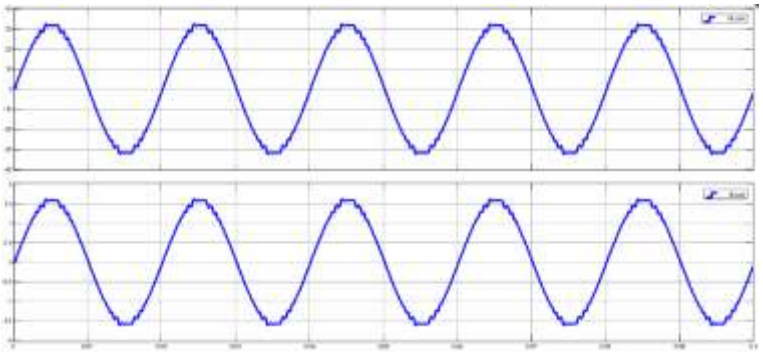

Figure 12. Simulation Result of Open-Loop Inverter

4.2 PI Controller

Simulink model of the PI controller-based current controller for the inverter is shown in Figure 13.

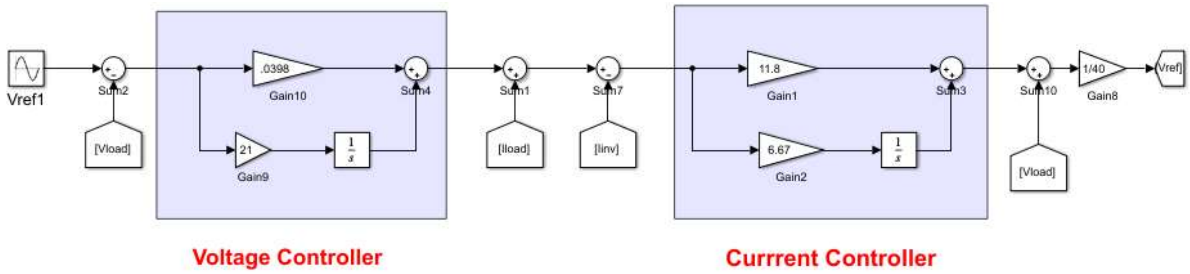

Figure 13. Simulink Model of PI Current Controller

The voltage of the grid and I_{grid} are in phase and have a pure sinusoidal waveform that approaches a power factor of one. Fig. 8 displays the PI control signal as well as the error signal (I_{ref} - I_{inv}). The V_{ref} control signal and the triangle carrier signal are compared to produce the inverter switches' switching pulses.
From figure 14, simulation of open loop inverter for DC voltage of 40V with 20 kHz as switching frequency is performed, and the output voltage obtained as 30V and current of 1.5A with 50Hz fundamental frequency. For this, the THD of the load current is given as 3.20%.

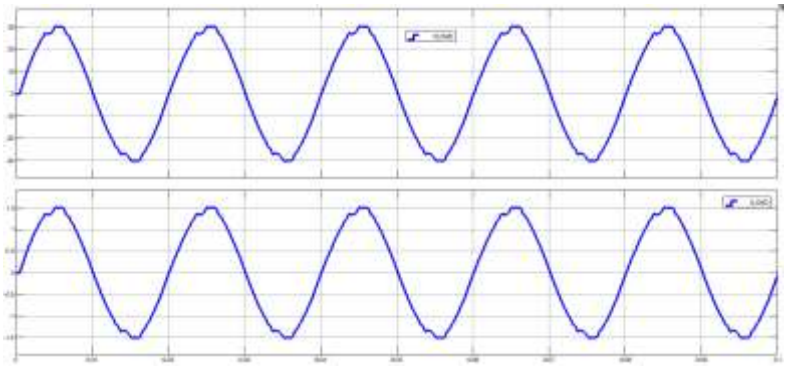

Figure 14. Simulation Result of Inverter with PI Current Controller

4.3 PR Controller

The PR controller simulation created with Simulink is displayed in Figure 15. The PR controller regulates the discrepancy between the reference current at the voltage controller and the inverter current I_{inv}.

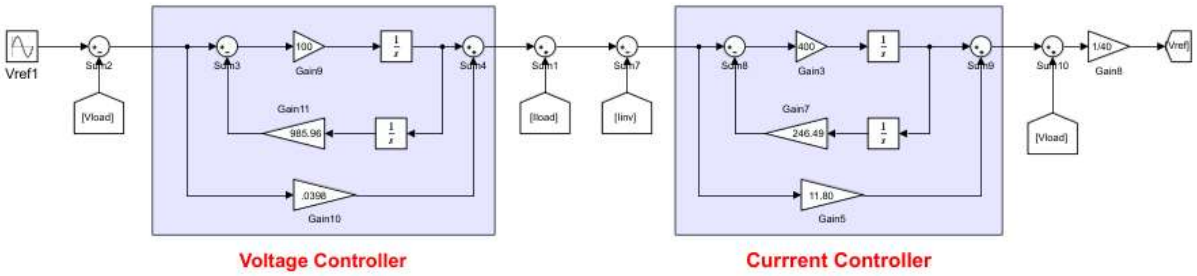

Figure 15. Simulink Model of PR Current Controller

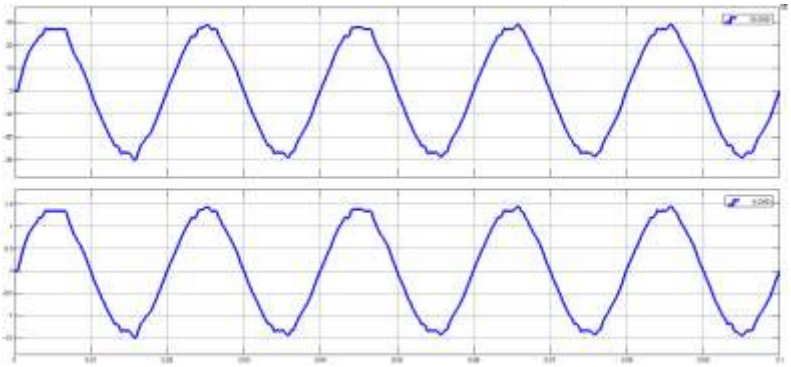

Figure 16. Simulation Result of Inverter with PR Current Controller

As shown in Figure 16, a unity power factor output is obtained in simulation with a 50Hz fundamental frequency as output frequency with 28.5V and 1.43A as output voltage and current, respectively.

4.4 PR with PLL

PLL is a phase-locked Loop, which uses two voltage components that are displaced by 90^0 realized using low-pass filters. The output obtained has a magnitude of 28.3V and 1.41A are the output voltage and current, respectively. Here, simulation is carried out by taking 20 kHz as the switching frequency with 40 V as the input DC voltage. Figure 17 shows the active power control of the inverter using PR with PLL.

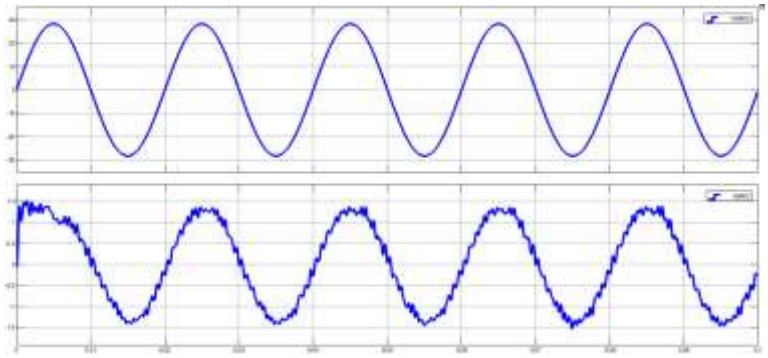

Figure 17. Simulation Result of Inverter with PR with PLL Current Controller

4.5 DQ Controller

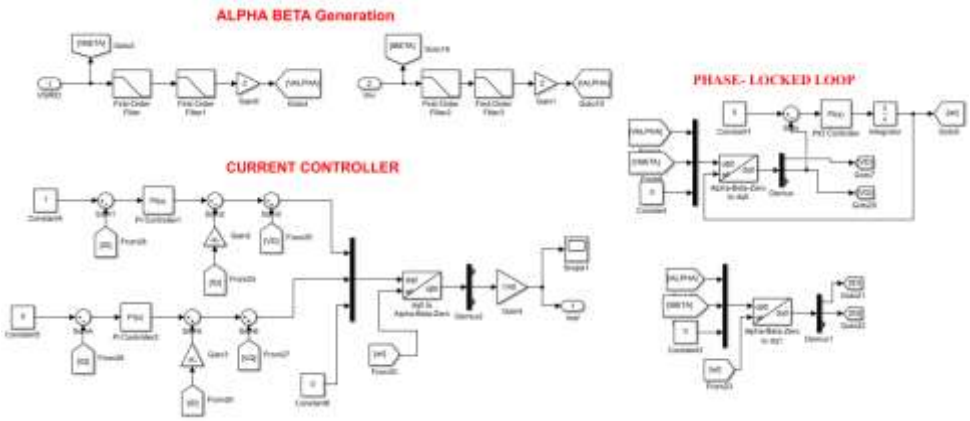

Figure 18. Simulink Model of DQ Current Controller

Fig. 18 shows the Simulink model of the DQ current controller. The injected grid current and, therefore, the inverter current will increase as the grid voltage falls [2].

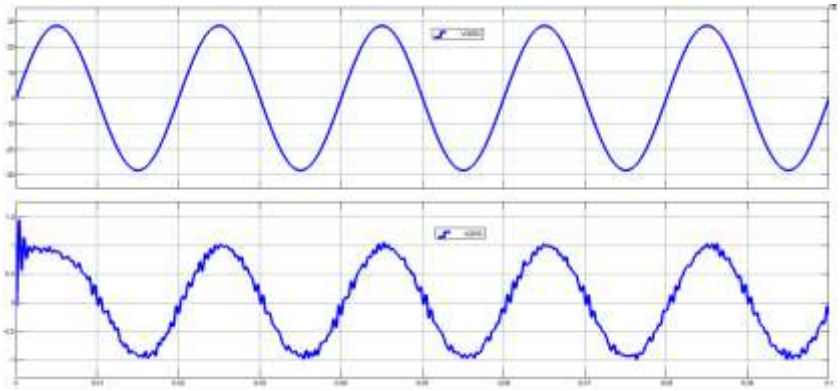

Figure 19. Simulation Result of Inverter with DQ Current Controller

4.6 Hysteresis Controller

4.6.1 Single Band Hysteresis Controller

Simulink model of the hysteresis controller for a switching frequency of 20 kHz is shown in Figure 20.

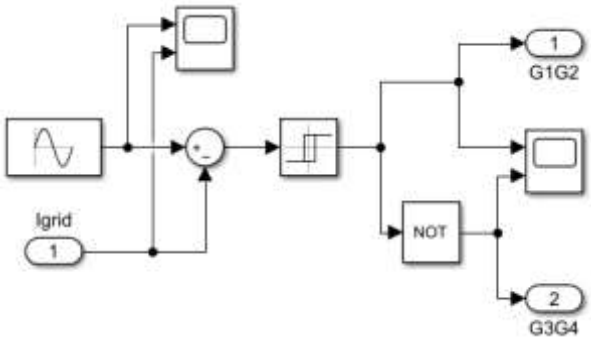

Figure 20. Simulink Model of Hysteresis Current Controller

As in equation 12, for a 20 kHz switching frequency hysteresis band is selected as 0.27. Simulation result using 0.27 as the band is plotted in Figure 21 with the current THD of 3.19%.

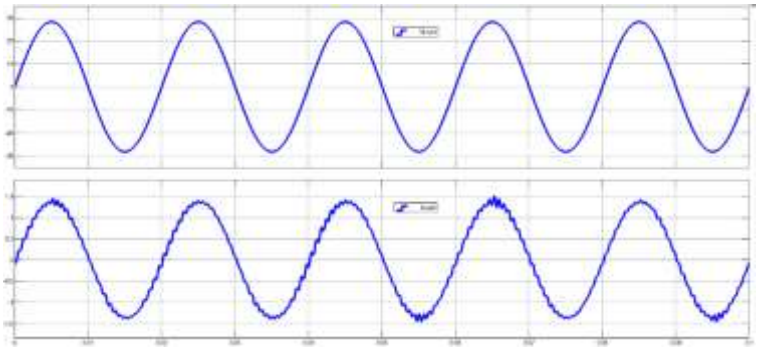

Figure 21. Simulation Result of Single-band Hysteresis Current Controller

4.6.2 Double Band Hysteresis Controller Method 1 (DBHCC 1)

Figure 22 shows the simulation results for the double band hysteresis controller. A smaller hysteresis band governs a set of switches in the single-phase inverter leg, while a bigger hysteresis band governs a second

set of switches.

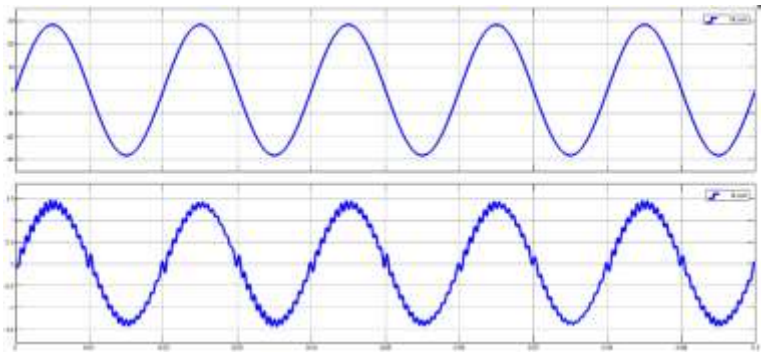

Figure 22. Simulation Result of Double band Hysteresis Controller method 1

4.6.3 Double Band Hysteresis Controller Method 2 (DBHCC 2)

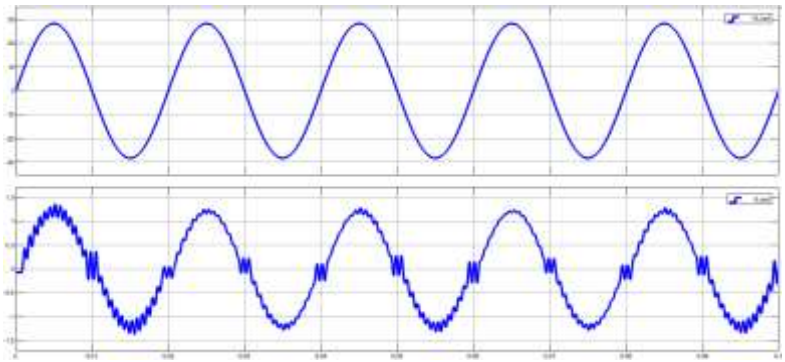

Figure 23. Simulation Result of Double band Hysteresis Current Controller method 2

The simulation results for the double band hysteresis controller type 2 with a unipolar output voltage scheme are displayed in Figure 23.

4.7 Total Harmonic distortion of Hysteresis current controller

For all varieties of hysteresis controllers, the switching frequency changed by the hysteresis band, as shown by the formulae. A grid-connected inverter with a variable hysteresis band is subjected to comparisons between multiple hysteresis techniques, as shown in Table 2, and the related switching frequency and THD are computed. The greatest frequency of switching at which an inverter can function for a certain combination of the inductance and source determines which HB should be used.

Table 2 shows the result of %THD versus bandwidth for SBHCC. From the table, we can get a lower THD with 0.1 as a hysteresis band for a switching frequency of 53.19 kHz.

Table 2. %THD versus Bandwidth for SBHCC

SBHCC		
Hysteresis Band	**Switching Frequency in kHz**	**THD%**
0.1	53.19	1.93
0.25	21.3	2.94
0.27	20	3.19
0.5	10.6	4.14
0.75	7.1	94.8

Table 3 shows the variation of THD for different values of hysteresis band for double band hysteresis controller type1. As band value increases THD also increases. Switching frequency goes down as listed in table. Higher switching frequency is obtained as 70.9 kHz for 0.05 band and corresponding THD as 1.69%. Similarly, lower switching frequency 4.7 kHz is occurred at 0.75 band at THD of 83.6%.

Table 3. %THD versus Bandwidth for DBHCC method 1

DBHCC- method 1		
Hysteresis Band	**Switching Frequency in kHz**	**THD%**
0.05	70.9	1.69
0.1	35.5	6.05
0.18	20	8.01
0.25	14.19	10.97
0.5	7.09	21.27
0.75	4.7	83.6

Table 4. %THD versus Bandwidth for DBHCC method 2

DBHCC- method 2		
Hysteresis Band	**Switching Frequency in kHz**	**THD%**
0.05	141.8	1.68
0.1	70.92	5.16
0.25	28.37	10.96
0.35	20	13.98
0.5	14.18	21.86
0.75	9.46	32.7

Variation of double band hysteresis current controller type 2 for various hysteresis bands is listed in Table 4. The lowest THD of 1.68% is obtained for the 0.05 band with 141.8 kHz, and a THD of 32.7% for the 0.75 band with 9.46 kHz switching frequency. For 20 kHz corresponding THD obtained is 13.98% for a hysteresis band of 0.35.

4.8 %THD versus current controllers

Table 5. %THD for different current controllers for 20 kHz switching frequency

Inverter Current controllers		**%THD**
Without controller		2.55
PI Controller		3.20
PR Controller		3.05
DQ Controller		7.08
	Single banded	3.19

Hysteresis Controller	Double-banded Type 1	8.01
	Double-banded Type 2	13.98

Table 5 gives a variation of THD for a fixed switching frequency of 20 kHz for different current controllers explained earlier. All simulations are done for a 20-watt system with 1A load current with 40V DC input voltage. From Table 5, the lowest THD occurs for PR current controllers, and the highest THD occurs for the hysteresis current controller.

5. Conclusions

This study compares and analyses several current control methods for grid-connected inverters. The MATLAB/Simulink software is used to evaluate the effectiveness of the various methods. All currently employed control strategies attain a power factor of unity. Current THD and switching frequency are two important measures that are compared. Therefore, in terms of power quality and steady-state error, PI controllers are not as effective as PR controllers. To validate the features and operation of the suggested control, a MATLAB/Simulink simulation has been employed. Phase locked loops (PLL) are used to continuously lock the phase of the grid voltage to preserve the dq frame converted signals in synchronism with the grid. The performance of various hysteresis controllers in terms of switching frequency and THD is provided after evaluation for a range of HB values. For DBHCC-1, at 70.9 kHz at 0.05 A of HB, a minimal THD of 1.68% is obtained; at 4.7 kHz, a minimum switching frequency is discovered, but the THD increases. Next, several hysteresis controllers are investigated to determine the highest switching frequency for a range of HB.

References

1. P. Nithara and R. P. Eldho, "Comparative Analysis of Different Control strategies in Single phase Standalone Inverter," *2021 7th International Conference on Advanced Computing and Communication Systems (ICACCS)*, Coimbatore, India, 2021, pp. 1105-1109, doi: 10.1109/ICACCS51430.2021.9441547.
2. I. Jayathilaka *et al*., "DQ Transform Based Current Controller for Single-Phase Grid Connected Inverter," *2018 2nd International Conference On Electrical Engineering (EECon)*, Colombo, Sri Lanka, 2018, pp. 32-37, doi: 10.1109/EECon.2018.8541004.
3. J. K. Singh and R. K. Behera, "Hysteresis Current Controllers for Grid Connected Inverter: Review and Experimental Implementation," *2018 IEEE International Conference on Power Electronics, Drives and Energy Systems (PEDES)*, Chennai, India, 2018, pp. 1-6, doi: 10.1109/PEDES.2018.8707755.
4. S. Jena, B. C. Babu, A. K. Naik and G. Mishra, "Performance improvement of single-phase grid — Connected PWM inverter using PI with hysteresis current controller," *2011 International Conference on Energy, Automation and Signal*, Bhubaneswar, India, 2011, pp. 1-5, doi: 10.1109/ICEAS.2011.6147101.
5. J. Sedo and S. Kascak, "Control of single-phase grid connected inverter system," *2016 ELEKTRO*, Strbske Pleso, Slovakia, 2016, pp. 207-212, doi: 10.1109/ELEKTRO.2016.7512066.

6. H. Cha, T. -K. Vu and J. -E. Kim, "Design and control of Proportional-Resonant controller based Photovoltaic power conditioning system," *2009 IEEE Energy Conversion Congress and Exposition*, San Jose, CA, USA, 2009, pp. 2198-2205, doi: 10.1109/ECCE.2009.5316374.
7. M. Parvez, M. F. M. Elias and N. A. Rahim, "Performance analysis of PR current controller for single-phase inverters," *4th IET Clean Energy and Technology Conference (CEAT 2016)*, Kuala Lumpur, Malaysia, 2016, pp. 1-8, doi: 10.1049/cp.2016.1311.
8. N. S. Yusof and A. Z. Ahmad, "Single-Phase grid-connected of PV inverter using PR current controller," *2017 IEEE Conference on Systems, Process and Control (ICSPC)*, Meleka, Malaysia, 2017, pp. 117-121, doi: 10.1109/SPC.2017.8313032.
9. P. A. Dahono, "New current controllers for single-phase full-bridge inverters," *2004 International Conference on Power System Technology, 2004. PowerCon 2004.*, Singapore, 2004, pp. 1757-1762 Vol.2, doi: 10.1109/ICPST.2004.1460287.
10. S. Jena, B. Mohapatra and C. K. Panigrahi, "Realization of double band hysteresis current controller for single phase grid connected pulse width modulated voltage source inverter," *2015 International Conference on Man and Machine Interfacing (MAMI)*, Bhubaneswar, India, 2015, pp. 1-6, doi: 10.1109/MAMI.2015.7456579.
11. A. Nachiappan, K. Sundararajan and V. Malarselvam, "Current controlled voltage source inverter using Hysteresis controller and PI controller," *2012 International Conference on Power, Signals, Controls and Computation*, Thrissur, India, 2012, pp. 1-6, doi: 10.1109/EPSCICON.2012.6175247.
12. S. Jena, N. Tiwary, C. K. Panigrahi and P. K. Sahu, "Performance Improvement of Grid Integrated Voltage Source Inverter Using Different Hysteresis Current Controllers," *2020 IEEE 7th Uttar Pradesh Section International Conference on Electrical, Electronics and Computer Engineering (UPCON)*, Prayagraj, India, 2020, pp. 1-6, doi: 10.1109/UPCON50219.2020.9376436.
13. A. I. Putri, A. Rizqiawan, F. Rozzi, N. Zakkia, Y. Haroen and P. A. Dahono, "A hysteresis current controller for grid-connected inverter with reduced losses," *2016 2nd International Conference of Industrial, Mechanical, Electrical, and Chemical Engineering (ICIMECE)*, Yogyakarta, Indonesia, 2016, pp. 167-170, doi: 10.1109/ICIMECE.2016.7910446.
14. M. Chinnari, T. Mounika, K. Swetha, A. Bharathi and A. H. Chander, "Implementation of Hysteresis Voltage Control for Different Inverter Topologies," *2020 IEEE India Council International Subsections Conference (INDISCON)*, Visakhapatnam, India, 2020, pp. 272-277, doi: 10.1109/INDISCON50162.2020.00062.
15. S. Rhili, H. Trabelsi and J. Hmad, "PI and PR Current Controllers of Single Phase Grid Connected PV system : Analysis, Comparison and Testing," *2019 16th International Multi-Conference on Systems, Signals & Devices (SSD)*, Istanbul, Turkey, 2019, pp. 700-705, doi: 10.1109/SSD.2019.8893232.
16. G. Ganesan @ Subramanian, Dr.M.K.Mishra, K.Jayaprakash, "Simulation Study of Hysteresis Current Controlled Single Phase Inverters for Photovoltaic Systems with Reduced Harmonics level", *International Journal of Applied Engineering Research ISSN 0973-4562 Volume 13, Number 6 (2018)*
17. Trung-Kien Vu , Se-Jin Seong, "Comparison of PI and PR Controller Based Current Control Schemes for Single-Phase Grid-Connected PV Inverter", *International Journal of Electrical, Computer, Energetic, Electronic and Communication Engineering Vol:8, No:2, 2014.*
18. S. Chatterjee and S. Chatterjee, "Simulation of synchronous reference frame PLL based grid connected inverter for photovoltaic application," *2015 1st Conference on Power, Dielectric and Energy*

Management at NERIST (ICPDEN), Itanagar, India, 2015, pp. 1-6, doi: 10.1109/ICPDEN.2015.7084493.